Carbohydrate Polymers 90 (2012) 340–347

Contents lists available at SciVerse ScienceDirect

Carbohydrate Polymers

journal homepage: www.elsevier.com/locate/carbpol

Effects of heat-moisture treatment on normal and waxy rice flours and production of thermoplastic flour materials

Prapaisut Khamthong, Namfone Lumdubwong*

Department of Packaging and Materials Technology, Faculty of Agro-Industry, Kasetsart University, Bangkok 10900, Thailand

ARTICLE INFO

Article history:
Received 4 January 2012
Received in revised form 12 May 2012
Accepted 17 May 2012
Available online 26 May 2012

Keywords:
Heat-moisture treatment
Rice flour
Thermoplastic flour materials
Bio-based packaging

ABSTRACT

Different levels of heat-moisture treatment (HMT) were applied to normal and waxy rice flours. Changes in chemical composition and functional properties of both flours were investigated. It was found that HMT induced β-turn conformation of rice proteins. Levels of HMT and types of rice flour interactively influenced thermal properties and XRD patterns of flour. When heat-moisture treated flour was utilized for production of thermoplastic flour (TPF) materials, it was found that HMT improved continuity of injection molding, complete mold filling, and yielded homogenous TPF materials. HMT levels affected the mechanical, thermal and barrier properties of TPF resin and materials differently. The ratio of HMT level to native flours was proposed for use not only for resin processing and injection molding, but also for improving mechanical and barrier properties of TPF materials.

1. Introduction

Heat-moisture treatment (HMT) is a physical modification method which combines high temperature (84–120 °C) with intermediate moisture content (less than 35%), and is applied to starch for periods varying from 15 min to 16 h (Gunaratne & Hoover, 2002). Effects of HMT on starch structure, chemical components, and physicochemical properties have been reported by several studies (Adebowale, Henle, Schwarzenbolz, & Doert, 2009; Hoover & Manuel, 1996; Khunae, Tran, & Sirivongpaisal, 2007; Vermeylen, Goderis, & Delcour, 2006).

Types of starch and levels of HMT – determined by moisture content, heating temperature, and heating time – also influence changes in the structure of starches and their functional properties. HMT is known for decreasing the degree of starch crystallinity, and for altering the XRD pattern of starch from B-type to A- or C-type, as reported in legume, tuber and root starches (Adebowale et al., 2009; Jacobs & Delcour, 1998; Vermeylen et al., 2006). However, Watcharatewinkul, Puttanlek, Rungsardthong, and Uttapap (2009) reported that heat-moisture treated (*hmt*) canna starch retained its original B-type XRD pattern when modified under 25% moisture content at 100 °C for 16 h. Starch with A-type pattern either retained its original pattern or changed to a V-pattern after HMT, depending on HMT levels and types of starch (Shih, King, Daigle, An, & Ali, 2007).

In contrast with the number of reports on the effects of HMT on starch structure and functional properties, few studies have investigated the effects of HMT on flour structure and properties, and the utilization of HMT starches and flours. Miyazaki and Morita (2005) partially substituted *hmt* corn starch for wheat flour in order to improve bread quality and found that bread containing *hmt* starch had higher specific bread volume. The grain structure of the bread became finer, but the elasticity of bread dough decreased. Hormdok and Noomhorm (2007) reported that rice noodles produced from a mixture of native rice flour and *hmt* rice starch had higher values of tensile strength, hardness, and extensibility and less cooking loss than native rice flour noodles. Cham and Suwannaporn (2010) also reported that *hmt* rice noodles had high tensile strength, gel hardness, and cooking yield.

Since previous studies of utilization of *hmt* flour and starch suggested that HMT improved tensile strength, gel hardness, and extensibility of noodles, the materials containing intermediate to high water content. It is interesting to explore the potential uses of *hmt* materials containing limited water content. The issue of sustainability is currently of crucial importance, together with the quest for bio-based and renewable materials to replace petroleum-based materials. The objectives of this study, therefore, were to investigate utilization of *hmt* flour via production of thermoplastic flour (TPF) materials using extrusion and injection molding with different levels of *hmt* flour, and to examine thermal, mechanical and barrier properties of the *hmt* TPF materials. Effects of different levels of HMT on chemical composition and functional properties of normal and waxy flours were also explored. Normal and waxy rice flours were chosen as raw materials for the study.

* Corresponding author. Tel.: +66 02 562 5098; fax: +66 02 562 5046.
E-mail address: faginfl@ku.ac.th (N. Lumdubwong).

0144-8617/$ – see front matter
http://dx.doi.org/10.1016/j.carbpol.2012.05.049

2. Materials and methods

2.1. Materials

Native normal and waxy rice flours were purchased from Patum Rice Mill and Granary Company (Pathum Thani, Thailand). Distilled water, a commercial-grade glycerol product, and analytical-grade chemicals were used in the study unless otherwise noted.

2.2. Heat-moisture treatment

Normal and waxy rice flours were heat-moisture treated using a modified method of Gunaratne and Hoover (2002). The flour moisture content was brought to 20% and 30%, respectively. Flour samples were then quickly transferred to glass jars and tightly sealed. All samples were heated in a hot-air oven (FD 53; Binder GmbH, Germany) at 100 °C and 120 °C for 4 and 16 h. Later, the sample-containing jars were opened and the samples were cooled down at ambient temperature (30 ± 3 °C). The *hmt* flours were then spread evenly ~2 cm thick on aluminum trays and dried in a hot-air oven at 40 °C to the moisture content of 10–12%. Later, the *hmt* flour samples were passed through a 100-mesh sieve and kept in polypropylene bags at ambient temperature.

2.3. Preparation of thermoplastic resin from native and hmt rice flours

A 2^3 experiment – which included moisture content (MC), 20% and 30%; heating temperature, 100 °C and 120 °C; and time, 4 and 16 h – was used in the study. Only waxy rice flour (WRF) was heat-moisture treated using the mentioned conditions. The *hmt* flour was mixed thoroughly with native normal rice flour at a weight ratio of 70:30 using a ribbon mixer (Reliance Tech-Service, Bangkok, Thailand) for 15 min. As a control, native waxy flour was mixed with native normal flour at a similar weight ratio. Glycerol was later added to the flour mixture at a ratio of 23:77 (wet basis), and the sample was mixed further for 15 min. Afterwards, all samples were kept in polypropylene bags overnight at ambient temperature. Each sample was manually fed into a co-rotating twin-screw extruder (LTE-20-40; Labtech Engineering Co. Ltd., Samut Prakan, Thailand) with L/D = 40 and a screw speed of 170 rpm. The temperature profile along the extruder barrel ranged from 110 °C to 125 °C (from feed zone to die). The extrudates were cut by a pelletizer (LZ-120, Labtech Engineering), yielding 3-mm pellets. Thermoplastic flour (TPF) resins were oven-dried at 60 °C overnight. The dried pellets were stored in polypropylene bags at ambient temperature in desiccators containing silica gels.

2.4. Bio-based sheet, dumbbell, and rigid packaging production from TPF resins

TPF resins were dried at 60 °C until their final moisture content was 3.0–3.5% by weight prior to production of sheet, dumbbell, and rigid packaging. To produce bio-based sheet, the resins were manually fed into the abovementioned co-rotating twin-screw extruder with a flat die at a screw speed of 145–150 rpm. The die gap was 1 mm with a sample feed rate of 3.2–4.0 rpm. The temperature profile along the extruder barrel was similar to that of TPF resin production. The extruder was attached to a laboratory benchtop chill roll cast film and sheet extrusion line (LBCR-150, Labtech Engineering). The chill roll temperature was 30 °C and the speeds of the chill roll sets were 0.5 and 0.3 m/min, respectively.

TPF resins were manually fed into an injection molding machine (BA 250 CDC; Battenfeld, Austria). The temperature profile of the barrel from feed zone to die ranged from 170 to 120 °C. The mold temperature was set at 17 °C and the injection speeds ranged from 112 to 270 rpm. Maximum injection pressures and cooling times were 55–95 bar and 45 s.

For further analysis, TPF resins and sheets were kept in desiccators containing silica gels at ambient temperature for not more than two weeks.

2.5. Characterizations of native and hmt rice flours and thermoplastic flour materials

All measurements were performed with at least two replicates unless otherwise stated. Moisture, ash, and crude fat contents were determined using AACC methods (AACC method 44-15A and AACC method 08-01) and a Soxtec system (HT 220 extraction unit, Tecator, Herndon, VA), respectively. Nitrogen content was measured by the Kjeldahl method and converted to protein content using a conversion factor of 5.95 (AACC method 46-13). Apparent and absolute amylose contents (AAM and AbAM) of native and *hmt* flours were determined by the iodine binding method of Chrastil (1987). Flour samples were defatted prior to the AbAM measurement using the method of Hoover and Ratnayake (2001).

Raman spectra of native and *hmt* samples were recorded with a Fourier transform Raman spectrometer (Spectrum GX; PerkinElmer, USA) with an Nd:YAG laser emitting at 1064 nm as the excitation source. The laser energy was set at 500 mW and scans were taken from 3500 to 200 cm^{-1}.

The color of flour samples was determined with a Miniscan™ XE spectrophotometer (Hunter Associates Laboratory, USA). Water absorption capacity of the samples was measured using the method of Beuchat (1997).

The modified method of Singh, Okadome, Toyoshima, Isobe, and Ohtsubo (2000) was used to determine thermal properties of native and *hmt* flours (~11% moisture) and TPF resins (~3% moisture). Thermal transitions of the samples were measured using a DSC 882e differential scanning calorimeter (Mettler-Toledo, Greifensee, Switzerland). The samples were heated from 0 °C to 250 °C at 10 °C/min.

Glass transition temperatures (T_gs) of TPF resins with 5 mm diameter and 4 mm height were also analyzed using an Eplexor® dynamic mechanical analyzer (GABO Qualimeter, Germany). The static load and dynamic load were 30 N and 15 N, respectively; the maximum static strain and dynamic strain were set at 0.4% and 0.2%. The test was performed in compression mode at a frequency of 1 Hz and a temperature range from −100 °C to 120 °C with a heating rate of 5 K/min.

Thermal degradation of native and *hmt* flour samples and TPF resins was determined with a thermal gravimetric analyzer (STA PT1000; Linseis, Germany). Each flour and resin sample (~10 mg) was placed in a crucible and heated from 30 °C to 800 °C at 10 °C/min in nitrogen atmosphere.

Crystallinity of native and *hmt* flour samples was analyzed using an X-ray diffractometer, model PW 1830 (Philips, The Netherlands). The diffractograms were measured at Bragg's angle (θ) from 5 to 35 °C at 3 °C/min operating at 40 kV and 30 mA.

The melt flow index (MFI) of TPF resins was measured using a Melt Flow Indexer (Dynisco, USA) according to ASTM standard method D1238-04 at a temperature of 190 °C and 2.16 kg load. The preheating time was set to 6 min.

2.6. Mechanical and barrier properties of TPF materials

All dumbbell and sheet samples from native and *hmt* rice flours were stored in a closed chamber containing saturated magnesium nitrate solution at 30 °C (50% RH) for 2 d prior to mechanical and barrier testing. Tensile strength and percent of elongation of the samples were measured using ASTM standard method D638-03. An M350-5 electronic tensile strength meter (Testometric Co. Ltd., UK)

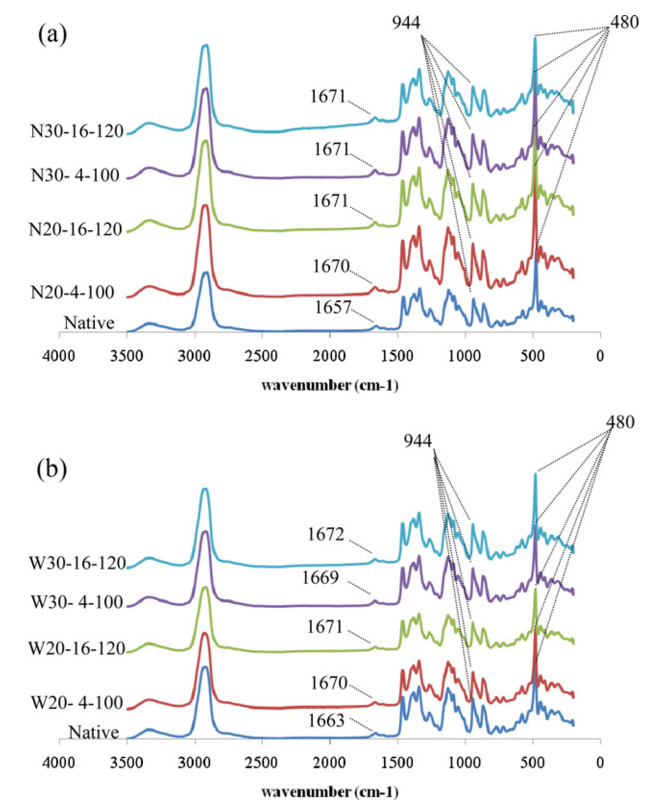

Fig. 1. FTIR spectra of: (a) native and *hmt* normal rice flour; (b) native and *hmt* waxy rice flour.

with a 5 kN load cell was used in the analyses. The testing crosshead testing speed was 50 mm min^{-1}; grip separation and gauge length were 100 mm and 50 mm, respectively.

Water vapor transmission rates (WVTR) and oxygen transmission rates (OTR) of thermoplastic rice flour sheets were measured using ASTM standard method E96/E96M-05 and ASTM standard method D3985-02, respectively.

2.7. Statistical analysis

All tests were performed at least in duplicate. Statistical significance tests were performed using Duncan's multiple range test at a 95% confidence level ($p < 0.05$).

3. Results and discussion

3.1. Chemical compositions and physicochemical properties of native and hmt flours

All HMT levels significantly increased both AAM (15–34%) and AbAM (30–69%) of normal rice flour (NRF) compared to native flour. In contrast, the values of AAM and AbAM of *hmt* waxy rice flour were the same as the native (Table 1). The results suggested that HMT affected starch in normal and waxy rice flours differently. HMT likely increases the availability of the amylose to the iodine-binding assay. In addition, fat content of all *hmt* samples was found to be lower than the native, which is in agreement with the results of Adebowale, Olu-Owolabi, Olawumi, and Lawal (2005).

Wavenumbers of 480 and 944 cm^{-1} of FTIR spectra (Fig. 1a and b) indicated stretching vibration of the carbonated skeleton of the starch component (Piot, Autrant, & Manfait, 2000) in native and *hmt* flours. The peaks of the amide I spectral region (1700–1600 cm^{-1}), representing the secondary structure protein conformation of native NRF and WRF, were at frequencies of 1657

Table 1
Amylose content and physical properties of native and heat-moisture treated non-waxy (N) and waxy (W) rice flours.

Flour[a]	Amylose content (%)				Fat (%)		Color						Water absorption capacity	
	Apparent		Absolute				L		a^*		b^*		Residual water (ml/g)	
	N	W	N	W	N	W	N	W	N	W	N	W	N	W
Native	18.38[c]	2.17[a]	20.26[d]	1.45[a]	0.20[a]	0.39[a]	97.94[a]	97.88[a]	−0.25[c]	−0.36[e]	2.71[e]	4.69[e]	10.16[a]	10.10[a]
HMT20-4-100[b]	22.16[b]	2.07[a]	26.68[c]	1.19[a]	0.06[c]	0.12[b]	97.97[a]	96.87[b]	−0.10[c]	−0.03[d]	4.48[d]	7.18[d]	9.52[a]	9.24[c]
HMT20-16-120	24.66[a]	1.74[a]	31.17[ab]	1.91[a]	0.09[bc]	0.14[b]	93.05[b]	93.95[d]	1.79[b]	1.58[b]	10.08[b]	11.86[b]	9.23[ab]	8.85[d]
HMT30-4-100	21.15[b]	2.02[a]	28.98[bc]	2.01[a]	0.09[bc]	0.08[b]	97.12[a]	95.61[c]	0.04[c]	0.25[c]	5.71[c]	9.02[c]	8.35[bc]	8.44[e]
HMT30-16-120	21.24[b]	2.10[a]	34.28[a]	1.87[a]	0.10[b]	0.13[b]	90.11[c]	92.83[e]	3.03[a]	2.16[a]	12.54[a]	12.99[a]	7.51[c]	9.49[b]

Different superscripts on the same row are significantly different ($p < 0.05$).
[a] Protein and ash contents of native non-waxy and waxy rice flours were 10.0%, 0.5%, 8.5%, and 0.3%, respectively.
[b] HMTxx-yy-zzz is heat-moisture treated flour: xx = % moisture content; yy = heating time (h); and zzz = heating temperature (°C) (e.g. HMT20-4-100 is HMT flour using 20% moisture content, 4 h of heating time, and at 100 °C).

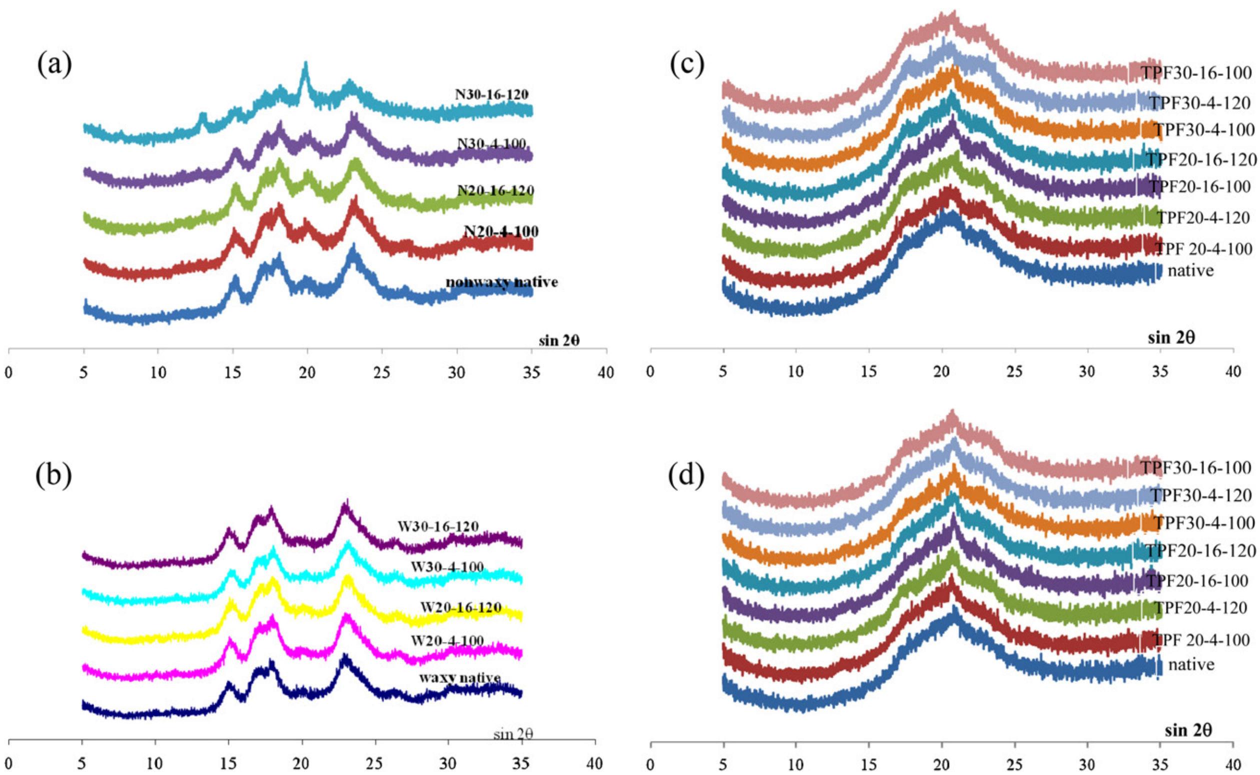

Fig. 2. X-ray diffraction patterns of: (a) native and *hmt* NRF; (b) native and *hmt* WRF; (c) TPF resin; (d) TPF materials.

and 1663 cm^{-1}; this implies that the secondary structures of the protein samples were α-helix and β-turn, respectively (Zeng, Cai, Cai, Wang, & Li, 2011). The peak of the amide I region of both flours was shifted to ~1670 cm^{-1}, the β-turn conformation, after the samples were heat-moisture treated (Fig. 1).

The redness ($a^* > 0$) and yellowness ($b^* > 0$) of *hmt* samples increased significantly, especially for the samples treated with high temperature and long heating time (Table 1). Evidently, non-enzymatic browning from the Maillard reaction and caramelization occurred in *hmt* samples. This effect was stronger in NRF samples than WRF samples since the a^* and b^* values of *hmt* NRF were much higher than those of the native NRF, compared to those values of *hmt* WRF and the native WRF. In addition, water absorption capacity (WAC) of *hmt* flour samples significantly increased. The incidence of high WAC was probably due to an increased amount of degraded starch, a diminishing amount of α-helix, the 2° protein conformation mentioned earlier, and also changes in the types and/or levels of biopolymer crystallinity from HMT, as discussed below.

3.2. Microstructure and thermal properties of hmt and native rice flours

All *hmt* and native flours displayed an A-type X-ray diffraction pattern, except the N30-16-120 sample whose pattern was clearly changed to V type (Fig. 2a and b). Levels of HMT possibly caused different arrangements of ordered starch molecules in NRF and WRF. Likely, HMT did not completely destroy the preexisting crystallinity of amylopectin (AP), but partially changed the degree of order of AP molecules, resulting in a shift of peak temperature (T_p) (Table 2). However, the most severe level of HMT influenced amylose–lipid complex formation in NRF, shown as two additional peaks at 13° and 20° (2θ), i.e. a V-type pattern, similar to the results of Khunae et al. (2007) and Shih et al. (2007).

Three thermal transitions were reported for native and *hmt* rice flours (Table 2 and Fig. 3a). Native NRF and WRF displayed similar T_{g1} (~55 °C), a little lower than previously reported (58 °C) by Cham and Suwannaporn (2010). HMT decreased T_{g1} of NRF, while the N20-16-120 sample possessed the lowest T_{g1} (44.3 °C). However, a similar trend was not found in *hmt* WRFs. Although most *hmt* WRFs had significantly lower T_{g1} compared to native WRF, the W30-16-120 sample displayed the lowest T_{g1} (48.3 °C), while the W20-4-100 flour had higher T_{g1} (77.1 °C) than the native. HMT generally increased the molecular mobility of the amorphous compounds in both normal and waxy samples. However the HMT20-4-100 condition, the lowest level of HMT, could decrease the molecular mobility of those compounds only in WRF. Likewise, levels of HMT and types of rice flour differently influenced T_m of samples. Most conditions of HMT decreased T_p of NRFs and WRFs. Nonetheless, HMT20-4-100 and the HMT30-16-120 caused increased T_p of NRF and WRF of approximately 15 °C and 7 °C, respectively (Table 2). The second T_g (T_{g2}) of *hmt* and native rice samples ranged from 200.7 °C to 220.9 °C, as reported by Singh et al. (2000). Once more, levels of HMT and types of flour affected T_{g2} of those samples differently and HMT seemingly tended to have more effect on changes in T_{g2} of waxy rice samples than normal rice samples (Table 2). Singh et al. (2000) suggested that cross-linking between starch and protein or fat (or both) increased T_g of native and *hmt* rice samples; whereas Chung, Woo, and Lim (2004) explained that increases in the free volume of polymers decreased T_g of the samples. Possibly both events occurred during HMT; but which one was dominant depended on levels of HMT, types of polymer, and chemical components of flour.

The thermal decomposition profiles of native and *hmt* rice flours displayed three peak temperatures with average mass loss of 10.5%, 66.5% and 20.5%, respectively (Fig. 3b and Table 2). The first step of mass loss was likely attributed to dehydration of samples (Riva, Fessas, & Schiraldi, 2000), while the second and third steps corresponded to the decomposition of flour components. HMT did not

Table 2
Thermal properties of native and heat-moisture treated non-waxy and waxy rice flours in a limited water system.

Sample	Thermal transition[a] (°C)					Thermal decomposition[b]		
	T_{g1}	Melting temperature (T_m)			T_{g2}	T_{d1} (°C)	T_{d2} (°C)	T_{d3} (°C)
		T_o	T_p	T_e				
Non-waxy native	55.7^{b}	161.1^{bcd}	167.8^{c}	172.8^{ef}	219.9^{ab}	86.2^{a}	295.8^{c}	490.4^{cd}
N20-4-100	53.6^{b}	171.2^{a}	182.7^{a}	191.0^{a}	219.6^{abc}	90.6^{a}	296.2^{bc}	486.1^{d}
N20-16-120	44.3^{d}	157.4^{cde}	163.2^{d}	170.5^{fg}	219.4^{abc}	84.5^{a}	296.3^{bc}	516.2^{bcd}
N30-4-100	52.1^{bc}	154.9^{def}	161.9^{de}	165.5^{h}	217.3^{bc}	83.0^{a}	298.5^{b}	534.0^{abc}
N30-16-120	51.9^{bc}	148.4^{f}	158.4^{e}	168.0^{gh}	220.9^{a}	82.0^{a}	297.8^{bc}	557.2^{ab}
Waxy native	55.5^{b}	162.3^{bc}	170.1^{c}	177.2^{d}	213.3^{d}	84.8^{a}	306.6^{a}	539.0^{ab}
W20-4-100	77.1^{a}	154.3^{def}	167.5^{c}	181.3^{c}	202.1^{ef}	81.8^{a}	307.2^{a}	543.1^{ab}
W20-16-120	52.5^{bc}	153.8^{ef}	166.6^{c}	174.4^{de}	216.9^{c}	84.4^{a}	307.4^{a}	562.4^{ab}
W30-4-100	56.5^{b}	155.8^{cde}	161.9^{de}	167.4^{gh}	200.7^{f}	85.3^{a}	308.8^{a}	553.0^{ab}
W30-16-120	48.3^{cd}	167.2^{ab}	177.9^{b}	186.9^{b}	204.6^{e}	82.2^{a}	306.7^{a}	575.2^{a}

Different superscripts on the same row are significantly different ($p < 0.05$).
[a] Thermal transition: T_g (glass transition temperature); T_o (onset temperature); T_m (midpoint temperature); T_e (endset temperature).
[b] Thermal decomposition: T_d (decomposition temperature).

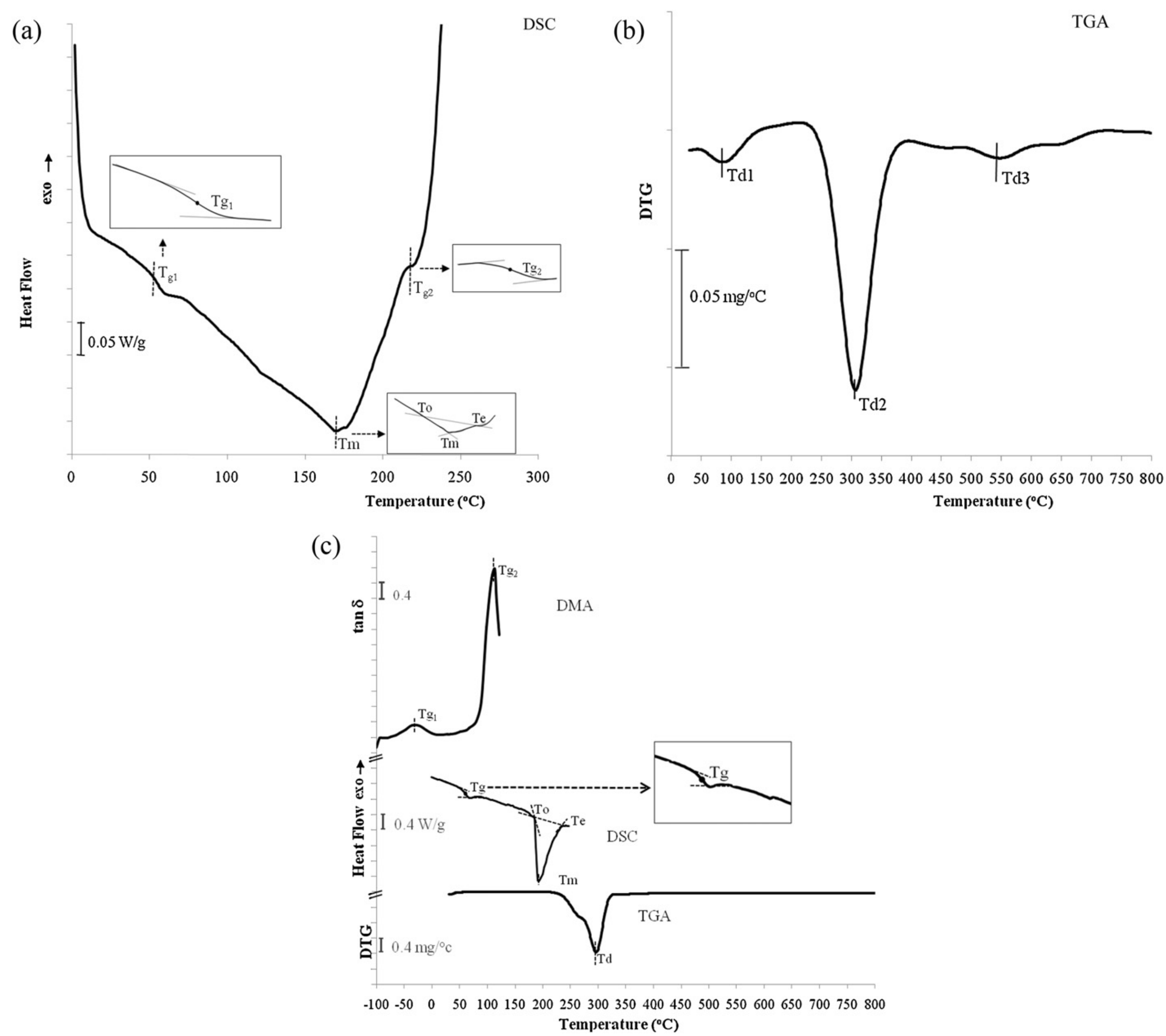

Fig. 3. (a) DSC thermogram of WRF; (b) DTG thermogram of WRF; (c) DSC and DTG thermograms and tan δ of TPF20-4-100 resin.

Table 3
Physical properties of thermoplastic flour resins from rice.

Sample	MFI (g/10 min)	DSC		DMA		TGA
		T_g (°C)	T_m (°C)	T_{g1} (°C)	T_{g2} (°C)	T_d (°C)
Native	3.82^{a}	56.98^{ns}	194.60^{ab}	-30.42^{ns}	93.52^{c}	292.60^{a}
TPF20-4-100	3.72^{a}	57.62^{ns}	194.08^{ab}	-30.20^{ns}	112.80^{a}	295.80^{a}
TPF20-4-120	1.64^{c}	53.36^{ns}	194.56^{ab}	-31.95^{ns}	105.40^{ab}	291.40^{a}
TPF20-16-100	2.54^{b}	53.34^{ns}	190.82^{abc}	-27.28^{ns}	106.25^{ab}	294.90^{a}
TPF20-16-120	1.50^{c}	55.99^{ns}	201.79^{a}	-29.52^{ns}	105.70^{ab}	292.80^{a}
TPF30-4-100	1.92^{bc}	54.22^{ns}	201.42^{a}	-24.62^{ns}	103.28^{b}	296.10^{a}
TPF30-4-120	2.00^{bc}	53.56^{ns}	175.76^{c}	-29.18^{ns}	110.88^{ab}	291.90^{a}
TPF30-16-100	2.56^{b}	59.45^{ns}	177.24^{bc}	-26.68^{ns}	105.78^{ab}	294.60^{a}

Different superscripts in the same row are significantly different ($p < 0.05$).

change T_{d2} of any normal and waxy rice samples, except for HMT N30-4-100. Nonetheless, all waxy flours had higher T_{d2} (~10 °C) and T_{d3} (~37 °C) than normal flours, indicating higher resistance to thermal decomposition. Aggarwal and Dollimore (1997) reported that AP and amylose (AM) possessed T_d of 325 °C and 315 °C. Therefore, a higher proportion of AP in waxy rice samples compared with normal samples (98% AP vs. 76–82% AP) may be the cause of higher T_d.

3.3. Thermoplastic resin production and thermal properties of thermoplastic flour (TPF) resin

Preliminary experiments showed that it is possible not only to produce resin from a mixture of both native NRF and WRF, but also from *hmt* flours. Nonetheless, a 70:30 (w/w) proportion of WRF and NRF was chosen for resin production in this study since the resin from the flour mixture at this fixed ratio improved continuity of the next processing step, injection molding. The authors found that TPF resin containing *hmt* WRF yielded completely formed specimens after injection molding (Fig. 4), whereas that from *hmt* NRF or from the resin containing both native normal and waxy rice yielded cracked specimens. In addition, the W30-16-120 flour sample was tremendously agglomerated and the lumps were very hard – a condition which is not practical for use in resin production. Consequently, the sample was omitted from resin and packaging production. Only seven levels of *hmt* WRF and native WRF mixed with native NRF at the ratio of 70:30 were used in the rest of the experiments.

The MFI of TPF resins ranged from 1.50 to 3.82 g/10 min (Table 3). All TPF resins produced from *hmt* WRF (except TPF20-4-100) had significantly lower MFI than that of native flour. The resins produced from waxy rice samples with 20% MC and treated at 120 °C heating temperature had the lowest MFI (~1.50–1.64 g/10 min), whereas the resins from waxy samples treated at 100 °C for 16 h yielded a range of MFI ~2.5 g/10 min.

Fig. 4. TPF resin and packaging.

All TPF resins displayed T_g ~ 55 °C and T_m ~ 177–202 °C, when analyzed by DSC (Fig. 3c). Once again, levels of HMT resulted in different T_m of TPF resins. Severity levels of HMT, especially with high MC, strongly affected a shift of T_m of TPF resins (Table 3). Thermal properties of the TPF resins were also analyzed using dynamic mechanical analysis (DMA). Two T_gs were reported. T_{g1} was ~−30 °C, which was the T_g of glycerol as suggested by Yokesahachert and Yoksan (2011). T_{g2} ranged from 93 °C to 112 °C, which was significantly higher than that determined by DSC, and signified chemical components of rice flours (likely starch and protein). The finding that T_g determined by DMA was higher than by DSC was due to dynamic and static measurements, as reported by Bengoechea, Arrachid, Guerrero, Hill, and Mitchell (2007). All *hmt* TPF resins had higher T_g than the native TPF resin. TPF20-4-100 and TPF30-4-100 resins had the highest and lowest T_g, respectively, among *hmt* TPF resins (Table 3). HMT, however, did not have any influence on T_d of TPF resin since all specimens displayed similar T_d of ~294 °C (Table 3).

3.4. Microstructure of TPF resin and injection molded materials

The diffraction pattern of TPF resins showed that the samples are semi-crystalline but primarily composed of amorphous regions, since the intensity of diffraction peaks was very low (Fig. 2c). TPF resins from all treatments showed a weak peak at $2\theta = 21°$. Also, low shoulders at $2\theta = 18°$ and 23° were found in some TPF resins, indicating a V+A-type pattern (Shih et al., 2007). The injection molding process amplified the V-type pattern in TPF materials, since all materials displayed a more pronounced peak at $2\theta = 21°$, compared to TPF resins (Fig. 2d). The V-type pattern in TPF resins and materials was likely not only from AM-lipid complexes, but the formation of AM-glycerol interaction (Corradini, de Carvalho, da Silva Curvelo, Agnelli, & Mattoso, 2007).

3.5. Mechanical and permeability properties of TPF materials from native and hmt rice flours

Mechanical properties of TPF materials are shown in Table 4. Percent elongation (E) of the materials was ~2.0–4.2%, exhibiting low ductility. Little differences were found between E at peak and E at break of each material while the stress values were different, indicating brittle fracture behavior for all the systems. Seemingly, MC of HMT had the most pronounced effect on the TS of all specimens, since all TPF materials containing *hmt* flour treated with 30% moisture had ~45% decrease in both TS at peak and TS at break. TPF 20-4-100 provided the best mechanical properties for rigid packaging production among all samples, since it exhibited the highest TS at peak, TS at break, and Young's modulus. The results show that a combination of HMT factors – interactions among MC, heating

Table 4
Mechanical and barrier properties of injection molded products from native and heat-moisture treated rice flours.

Sample	Mechanical properties					Barrier properties	
	Stress at peak (MPa)	Elongation at peak (%)	Stress at break (MPa)	Elongation at break (%)	Young's modulus (MPa)	WVP (cm^3 mm/m^2 d)	OP (cm^3 mm/m^2 d atm)
TPF native	14.40^{a}	3.80^{a}	9.40^{b}	3.84^{a}	363.80^{b}	12.81^{bcd}	50.25^{a}
TPF20-4-100	14.00^{a}	3.20^{b}	12.60^{a}	3.22^{b}	509.80^{a}	9.88^{e}	40.00^{bc}
TPF20-4-120	10.60^{b}	4.20^{a}	9.80^{ab}	4.23^{a}	321.80^{c}	15.07^{abc}	44.00^{ab}
TPF20-16-100	9.40^{c}	4.20^{a}	5.60^{cd}	4.23^{a}	290.80^{d}	12.44^{cd}	33.33^{c}
TPF20-16-120	10.80^{b}	4.00^{a}	7.40^{bc}	4.04^{a}	360.60^{b}	16.27^{a}	39.33^{bc}
TPF30-4-100	7.80^{d}	3.20^{b}	7.40^{bc}	3.24^{b}	277.60^{d}	15.98^{ab}	50.00^{a}
TPF30-4-120	6.00^{e}	2.00^{c}	5.00^{cd}	2.02^{c}	320.60^{c}	13.57^{abcd}	47.00^{ab}
TPF30-16-100	9.20^{c}	3.00^{b}	3.00^{d}	3.03^{b}	370.40^{b}	14.60^{abc}	49.33^{a}

Different superscripts in the same row are significantly different ($p < 0.05$).

temperature and heating time – influenced the mechanical properties of TPF materials. HMT can retain a high value of TS at peak and improve both TS at break and Young's modulus of the bio-based materials if the flour is physically modified at a "suitable" condition.

The extruded TPF sheet from different HMT conditions displayed thickness values of 0.20–0.42 mm. Only TPF 20-4-100 exhibited lower WVP as compared to other native and *hmt* materials (Table 4). It seems that other HMT, especially in the case of severe HMT conditions, slightly increased the WVP of TPF specimens.

Glycerol-plasticized starch films displayed good oxygen barriers if their moisture content was below 15% (Forssell, Lahtinen, Lahelin, & Myllarinen, 2002). TPF materials in the study also exhibited low oxygen permeability (OP). HMT at certain levels decreased OP, since TPF 20-4-100, TPF 20-16-100 and TPF 20-16-120 displayed better oxygen barrier properties than native and other *hmt* materials (Table 4).

The fact that HMT20-4-100 provided the best mechanical and improved barrier properties of TPF materials could possibly be due to free volume reduction and dedensification of the amorphous phase. The mildest HMT followed by resin processing and injection molding may cause mainly free volume reduction but the least dedensification, the effect which can decrease mechanical properties (Wang, Gupta, & Schiraldi, 2012), but increase oxygen permeability (Liu, Hu, Schiraldi, Hiltner, & Baer, 2004).

4. Conclusions

HMT induced β-turn conformation of rice proteins of normal and waxy rice flours. Levels of HMT and types of rice flour not only shifted the T_gs and T_m, but also influenced the XRD patterns. The ratio of *hmt* WRF to native NRF of 70:30 (w/w) was proposed as the proper ratio to use as material for resin processing and injection molding. Levels of HMT affected the thermal, mechanical and barrier properties of TPF resin and materials to varying degrees. TPF-20-4-100 exhibited the highest TS and Young's modulus, and relatively low WVP and OP compared to native and other *hmt* materials.

Acknowledgement

The authors would like to thank the National Research Council of Thailand (NRCT) for its support in funding this project.

References

AACC International. (2000). *Approved methods of analysis* (10th ed.). St. Paul, MN: American Association of Cereal Chemists.
Adebowale, K. O., Henle, T., Schwarzenbolz, U., & Doert, T. (2009). Modification and properties of African yam bean (*Sphenostylis stenocarpa* [Hochst. ex A. Rich.] Harms) starch. I. Heat moisture treatments and annealing. *Food Hydrocolloids*, *23*, 1947–1957.
Adebowale, K. O., Olu-Owolabi, B. I., Olawumi, E. K., & Lawal, O. S. (2005). Functional properties of native, physically and chemically modified breadfruit (*Artocarpus artilis*) starch. *Industrial Crops and Products*, *21*, 343–351.
Aggarwal, P., & Dollimore, D. (1997). The combustion of starch, cellulose and cationically modified products of these compounds investigated using thermal analysis. *Thermochimica Acta*, *291*, 65–72.
ASTM D1238-04. (2004). *Standard test method for melt flow rates of thermoplastics by extrusion plastometer*. Philadelphia, PA: American Society for Testing and Materials.
ASTM D3985-02. (2002). *Standard test method for oxygen gas transmission rate through plastic film and sheeting using a colorimetric sensor*. Philadelphia, PA: American Society for Testing and Materials.
ASTM D638-03. (2003). *Standard test method for tensile properties of plastics*. Philadelphia, PA: American Society for Testing and Materials.
ASTM E96/E 96M-05. (2005). *Standard test methods for water vapor transmission of materials*. Philadelphia, PA: American Society for Testing and Materials.
Bengoechea, C., Arrachid, A., Guerrero, A., Hill, S. E., & Mitchell, J. R. (2007). Relationship between the glass transition temperature and the melt flow behavior for gluten, casein and soya. *Journal of Cereal Science*, *45*, 275–284.
Beuchat, L. R. (1997). Functional and electrophoretic characteristics of succinylated peanut flour protein. *Journal of Agricultural and Food Chemistry*, *25*, 258.
Cham, S., & Suwannaporn, P. (2010). Effect of hydrothermal treatment of rice flour on various rice noodles quality. *Journal of Cereal Science*, *51*, 284–291.
Chrastil, J. (1987). Improved colorimetric determination of amylose in starches or flours. *Carbohydrate Research*, *159*, 154–158.
Chung, H.-J., Woo, K.-S., & Lim, S.-T. (2004). Glass transition and enthalpy relaxation of cross-linked corn starches. *Carbohydrate Polymers*, *55*, 9–15.
Corradini, E., de Carvalho, A. J. F., da Silva Curvelo, A. A., Agnelli, J. A. M., & Mattoso, L. H. C. (2007). Preparation and characterization of thermoplastic starch/zein. *Materials Research*, *10*, 227–231.
Forssell, P., Lahtinen, R., Lahelin, M., & Myllarinen, P. (2002). Oxygen permeability of amylose and amylopectin films. *Carbohydrate Polymers*, *47*, 125–129.
Gunaratne, A., & Hoover, R. (2002). Effect of heat-moisture treatment on the structure and physicochemical properties of tuber and root starches. *Carbohydrate Polymers*, *49*, 425–437.
Hoover, R., & Manuel, H. (1996). The effect of heat-moisture treatment on the structure and physicochemical properties of normal maize, waxy maize, dull waxy maize and amylomaize V starches. *Journal of Cereal Science*, *23*, 153–162.
Hoover, R., & Ratnayake, W. S. (2001). Determination of total amylose content of starch. In R. E. Wrolstad (Ed.), *Current protocols in food analytical chemistry*. Hoboken, NJ: John Wiley & Sons.
Hormdok, R., & Noomhorm, A. (2007). Hydrothermal treatments of rice starch for improvement of rice noodle quality. *LWT-Food Science and Technology*, *40*, 1723–1731.
Jacobs, H., & Delcour, J. A. (1998). Hydrothermal modifications of granular starch, with retention of the granular structure: A review. *Journal of Agricultural and Food Chemistry*, *46*, 2895–2905.
Khunae, P., Tran, T., & Sirivongpaisal, P. (2007). Effect of heat-moisture treatment on structural and thermal properties of rice starches differing in amylose content. *Starch/Starke*, *59*, 593–599.
Liu, R. Y. F., Hu, Y. S., Schiraldi, D. A., Hiltner, A., & Baer, E. (2004). Crystallinity and oxygen transport properties of PET bottle walls. *Journal of Applied Polymer Science*, *94*, 671–677.
Miyazaki, M., & Morita, N. (2005). Effect of heat-moisture treated maize starch on the properties of dough and bread. *Food Research International*, *38*, 369–376.
Piot, O., Autrant, J.-C., & Manfait, M. (2000). Spatial distribution of protein and phenolic constituents in wheat grain as probed by confocal Raman microspectroscopy. *Journal of Cereal Science*, *32*, 57–71.
Riva, M., Fessas, D., & Schiraldi, A. (2000). Starch retrogradation in cooked pasta and rice. *Cereal Chemistry*, *77*, 433–438.
Shih, F., King, J., Daigle, K., An, H.-J., & Ali, R. (2007). Physicochemical properties of rice starch modified by hydrothermal treatments. *Cereal Chemistry*, *84*, 527–531.
Singh, V., Okadome, H., Toyoshima, H., Isobe, S., & Ohtsubo, K. (2000). Thermal and physicochemical properties of rice grain, flour and starch. *Journal of Agricultural and Food Chemistry*, *48*, 2639–2647.

Vermeylen, R., Goderis, B., & Delcour, J. A. (2006). An X-ray study of hydrothermally treated potato starch. *Carbohydrate Polymers*, *64*, 364–375.

Wang, Y., Gupta, M., & Schiraldi, D. A. (2012). Oxygen permeability in thermoplastic polyurethanes. *Journal of Polymer Science Part B: Polymer Physics*, *50*, 681–693.

Watcharatewinkul, Y., Puttanlek, C., Rungsardthong, V., & Uttapap, D. (2009). Pasting properties of a heat-moisture treated canna starch in relation to its structural characteristics. *Carbohydrate Polymers*, *75*, 505–511.

Yokesahachert, C., & Yoksan, R. (2011). Effect of amphiphilic molecules on characteristics and tensile properties of thermoplastic starch and its blends with poly(lactic acid). *Carbohydrate Polymers*, *83*, 22–31.

Zeng, H.-Y., Cai, L.-H., Cai, X.-L., Wang, Y.-J., & Li, Y.-Q. (2011). Structure characterization of protein fractions from lotus (*Nelumbo nucifera*) seed. *Journal of Molecular Structure*, *1001*, 139–144.